Towards nonlinear conversion from mid- to near-infrared wavelengths using Silicon Germanium waveguides

Kamal Hammani,[1,5] Mohamed A. Ettabib,[1] Adonis Bogris,[2,3] Alexandros Kapsalis,[2] Dimitris Syvridis,[2] Mickael Brun,[4] Pierre Labeye,[4] Sergio Nicoletti,[4] and Periklis Petropoulos [1,*]

[1]*Optoelectronics Research Centre, University of Southampton, Highfield, Southampton, SO17 1BJ, United Kingdom*
[2]*Department of Informatics and Telecommunications, National and Kapodistrian University of Athens, Panepistimiopolis, Ilissia, 15784, Athens, Greece*
[3]*Department of Informatics, Technological Educational Institute of Athens, Aghiou Spiridonos, 12210 Egaleo, Athens, Greece*
[4]*CEA-Leti MINATEC Campus, 17 rue des Martyrs 38054 Grenoble Cedex 9, France*
[5]*Now at Laboratoire Interdisciplinaire Carnot de Bourgogne (ICB), UMR 6303 CNRS-Université de Bourgogne, 9 av. A. Savary, BP 47 870, F-21078 Dijon Cedex, France*
[*]*pp@orc.soton.ac.uk*

Abstract: We demonstrate the design, fabrication and characterization of a highly nonlinear graded-index SiGe waveguide for the conversion of mid-infrared signals to the near-infrared. Using phase-matched four-wave mixing, we report the conversion of a signal at 2.65 μm to 1.77 μm using a pump at 2.12 μm.

OCIS codes: (130.3120) Integrated optics devices; (160.4760) Optical properties; (190.4390) Nonlinear optics, integrated optics.

References and links

1. Y. Yao, A. J. Hoffman, and C. F. Gmachl, "Mid-infrared quantum cascade lasers," Nat. Photonics **6**(7), 432–439 (2012).
2. K. D. Buchter, M. C. Wiegand, H. Herrmann, and W. Sohler, "Nonlinear optical down- and up-conversion in PPLN waveguides for mid-infrared spectroscopy," in *CLEO Europe* (2009), paper CD_P8.
3. T. W. Neely, L. Nugent-Glandorf, F. Adler, and S. A. Diddams, "Broadband mid-infrared frequency upconversion and spectroscopy with an aperiodically poled LiNbO3 waveguide," Opt. Lett. **37**(20), 4332–4334 (2012).
4. B. Kuyken, X. Liu, R. M. Osgood, Jr., R. Baets, G. Roelkens, and W. M. J. Green, "Mid-infrared to telecom-band supercontinuum generation in highly nonlinear silicon-on-insulator wire waveguides," Opt. Express **19**(21), 20172–20181 (2011).
5. B. Kuyken, X. Liu, R. M. Osgood, Y. A. Vlasov, G. Roelkens, R. Baets, and W. M. J. Green, "Frequency conversion of mid-infrared optical signals into the telecom band using nonlinear silicon nanophotonic wires," in *Optical Fiber Communication Conference/National Fiber Optic Engineers Conference 2011*(Optical Society of America, 2011), paper OThU4.
6. N. K. Hon, R. Soref, and B. Jalali, "The third-order nonlinear optical coefficients of Si, Ge, and Si1-xGex in the midwave and longwave infrared," J. Appl. Phys. **110**(1), 011301 (2011).
7. M. A. Ettabib, K. Hammani, F. Parmigiani, L. Jones, A. Kapsalis, A. Bogris, D. Syvridis, M. Brun, P. Labeye, S. Nicoletti, and P. Petropoulos, "FWM-based wavelength conversion of 40 Gbaud PSK signals in a silicon germanium waveguide," Opt. Express **21**(14), 16683–16689 (2013).
8. K. Hammani, M. A. Ettabib, A. Bogris, A. Kapsalis, D. Syvridis, M. Brun, P. Labeye, S. Nicoletti, D. J. Richardson, and P. Petropoulos, "Optical properties of silicon germanium waveguides at telecommunication wavelengths," Opt. Express **21**(14), 16690–16701 (2013).
9. F. Li, S. D. Jackson, C. Grillet, E. Magi, D. Hudson, S. J. Madden, Y. Moghe, C. O'Brien, A. Read, S. G. Duvall, P. Atanackovic, B. J. Eggleton, and D. J. Moss, "Low propagation loss silicon-on-sapphire waveguides for the mid-infrared," Opt. Express **19**(16), 15212–15220 (2011).
10. J. D. Harvey, R. Leonhardt, S. Coen, G. K. L. Wong, J. C. Knight, W. J. Wadsworth, and P. S. J. Russell, "Scalar modulation instability in the normal dispersion regime by use of a photonic crystal fiber," Opt. Lett. **28**(22), 2225–2227 (2003).

#205974 - $15.00 USD Received 4 Feb 2014; revised 3 Apr 2014; accepted 3 Apr 2014; published 15 Apr 2014

11. S. Pitois and G. Millot, "Experimental observation of a new modulational instability spectral window induced by fourth-order dispersion in a normally dispersive single-mode optical fiber," Opt. Commun. **226**(1-6), 415–422 (2003).
12. P. Barritault, M. Brun, P. Labeye, O. Lartigue, J.-M. Hartmann, and S. Nicoletti, "Mlines characterization of the refractive index profile of SiGe gradient waveguides at 2.15 μm," Opt. Express **21**(9), 11506–11515 (2013).
13. Q. Lin, T. J. Johnson, R. Perahia, C. P. Michael, and O. J. Painter, "A proposal for highly tunable optical parametric oscillation in silicon micro-resonators," Opt. Express **16**(14), 10596–10610 (2008).
14. K.-D. F. Büchter, H. Herrmann, C. Langrock, M. M. Fejer, and W. Sohler, "All-optical Ti:PPLN wavelength conversion modules for free-space optical transmission links in the mid-infrared," Opt. Lett. **34**(4), 470–472 (2009).
15. S. P. Jung, Z. Sanja, M. Slaven, M. C.-B. Jose, B. D. Ivan, M. Shayan, and R. Stojan, "Mid-Infrared Four-Wave Mixing in Silicon Waveguides Using Telecom-Compatible Light Sources," in *Frontiers in Optics* (Optical Society of America, 2009), paper PDPB3.
16. S. Zlatanovic, J. S. Park, S. Moro, J. M. C. Boggio, I. B. Divliansky, N. Alic, S. Mookherjea, and S. Radic, "Mid-infrared wavelength conversion in silicon waveguides using ultracompact telecom-band-derived pump source," Nat. Photonics **4**(8), 561–564 (2010).

1. Introduction

The mid-infrared (mid-IR) spectral region has attracted a significant amount of interest in recent years. It contains the absorption "fingerprints" of most molecules of interest, thus suggesting several applications both in spectroscopy and chemical and biomolecular sensing. The recent development of mid-IR sources, most notably quantum cascade lasers (QCLs) [1], has further stimulated the interest of the research community in this area. However, the lack of small size, room temperature detectors exhibiting suitably high sensitivity at this wavelength region still remains an issue.

To overcome this difficulty, wavelength conversion of the mid-IR signals into the near-infrared (near-IR) is a promising alternative. This conversion can be done either through sum-frequency generation in a second-order nonlinear medium, such as periodically poled lithium niobate [2, 3], or through four-wave mixing (FWM) using a third-order nonlinear medium, such as silicon [4, 5]. Silicon is an excellent candidate for such applications, thanks to its transparency up to 8 μm, the reduced two-photon and free-carrier absorptions beyond 2 μm and its potential for monolithic integrated solutions. These features however, are not restricted to pure silicon. For instance, silicon germanium (SiGe) alloys have been identified as promising candidates for nonlinear applications in the midwave and longwave infrared thanks to their enhanced nonlinearity compared to pure Si [6]. Very recently [7, 8], we have demonstrated that $Si_{1-x}Ge_x$ waveguides also exhibit good wavelength conversion performance for all-optical processing applications at telecommunication wavelengths. Moreover, the germanium concentration, allows one additional free parameter in the tailoring of the waveguide's dispersion. Therefore, $Si_{1-x}Ge_x$ waveguides present themselves as an alternative CMOS-compatible platform for FWM-based optical processing.

In this paper, we demonstrate the nonlinear conversion of a mid-IR signal to the near-IR using a graded index SiGe waveguide specially designed for broadband conversion. A signal centered at 2.65 μm is converted to 1.77 μm using a pump centered at 2.12 μm. For the first time, broadband conversion via FWM is demonstrated in a SiGe waveguide.

2. Device description

2.1 Waveguide design

The SiGe device we used in our experiments was specifically designed for wavelength conversion from the mid- to near-IR. The $Si_{1-x}Ge_x$ compound offers continuous variation of the refractive index versus molar fraction. The specific SiGe platform also offers low propagation loss and efficient coupling with typical mid-IR sources, since SiGe allows matching the core/cladding index gap to that of QCLs [9]. The conversion was based on the FWM process pumped by a tunable and continuous wave (CW) source covering the 2 - 2.5 μm wavelength region. Therefore, the proposed waveguide should be able to carry the mid-IR

#205974 - $15.00 USD Received 4 Feb 2014; revised 3 Apr 2014; accepted 3 Apr 2014; published 15 Apr 2014

signal, the pump wave as well as the idler near-IR product at the same time while still maintaining (a) good mode confinement with a small effective mode area in order to give rise to intense nonlinear effects, (b) and low loss throughout the wavelength span.

In order to design the specific characteristics of the waveguide, we recalled the phase-matching condition for degenerate four-wave mixing in a waveguide, which is given by [4]:

$$\beta_2\omega^2 + \frac{\beta_4}{12}\omega^4 + 2\gamma P = 0 \qquad (1)$$

where β_2 and β_4 are the second- and fourth-order dispersion respectively at the pump frequency, $\gamma = n_2\omega/cA_{eff}$ is the nonlinear parameter of the considered waveguide which is a function of the nonlinear index n_2 and the effective mode area A_{eff}, P is the input power and ω is the frequency detuning between pump and signal. A consequence of Eq. (1) is that when $\beta_2 > 0$ (i.e. dispersion is normal) and $\beta_4 < 0$, there exist two gain bands in the spectrum. This is similar to modulation instability observed in anomalous dispersion, however in this case, the gain bands are narrower and located further away from the pump [10, 11].

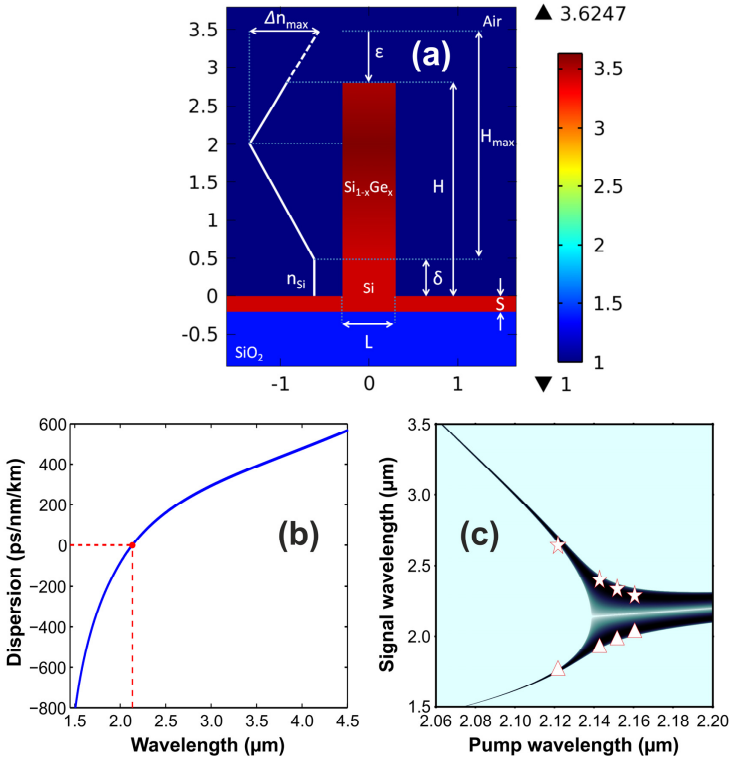

Fig. 1. (a) Graded index profile of the waveguide, (b) Estimated dispersion curve. The red point corresponds to zero dispersion wavelength. (c) Corresponding phase matching diagram. The white stars (resp. triangles) correspond to the signal (resp. idler) wavelengths leading to the best conversion efficiency experimentally.

Practically, the conversion efficiency will be maximum for an optimal wavelength defined as [11]:

$$\Omega_{opt} = \sqrt{\frac{2\sqrt{3\left(3\beta_2^2 - 2\beta_4\gamma P\right)}}{\beta_4} - 6\frac{\beta_2}{\beta_4}} \qquad (2)$$

#205974 - $15.00 USD Received 4 Feb 2014; revised 3 Apr 2014; accepted 3 Apr 2014; published 15 Apr 2014

It is then clear that the optimal wavelength depends strongly on β_2 and β_4, therefore the design of the waveguide is critical. In order to achieve the required dispersion characteristics, and a zero-dispersion wavelength (ZDW) close to the pump wavelength, i.e. around 2-2.5 μm, the contribution of waveguide dispersion needs to be significant and well-controlled. This can only be accomplished by strong modal confinement which implies a low-index surrounding and substrate material. A schematic of the cross-section of the waveguide is shown in Fig. 1(a). For the substrate, SiO_2 is a good candidate for our design, but any other Si-compatible low index material such as SiN_x, Al_2O_3 can also be used. In this work, we chose 200 mm SOI wafer with 2 μm buried oxide layers. Although SiO_2 is not transparent at wavelengths above 3 μm, recent results showed that its presence as a surrounding material in silicon on sapphire waveguides is not prohibitive for the achievement of low propagation loss in Si-based waveguides [9]. Additionally, the SiGe waveguide was designed to favor the TM polarization, to match that of the QCL sources that are commonly used in the mid-IR region.

On top of the low index substrate a continuous Si slab layer of thickness S = 210 nm was introduced [see Fig. 1(a)] under the nonlinear waveguide. The waveguide itself was constituted of a buffer with pure Si section of thickness δ surrounded by a SiGe section. This section exhibited a specific index profile, with a standard step index in the horizontal direction and a graded index profile in the vertical direction [9]. The step-index fiber-like behavior of the waveguide allows the centralization of the optical field in the high Ge region where the Kerr coefficient n_2 is higher, thus enhancing its nonlinear properties. The graded profile in the vertical direction (y) followed a symmetric double linear gradient, peaking in the middle of the distance ($H_{max} - \delta$). In the schematic, L denotes the waveguide width and H the total waveguide height after etching of the waveguide. H corresponds to the initial deposition height (H_{max}) reduced by the quantity ε after etching. The index would then normally vary from n_{Si} at y = δ to $n_{Si} + \Delta n_{max}$ at y = ($\delta + H_{max}$)/2 and then back down to n_{Si} at y = H_{max}. The maximum allowed Ge concentration at y = ($\delta + H_{max}$)/2 was 42%. Throughout the simulations H_{max} was kept constant at 3 μm. However, H (translating to a combination of ε and δ, since $H = \delta + H_{max} - \varepsilon$), L and S could be varied in order to properly engineer the waveguide's dispersion characteristics. The existence of a higher index core adjustable by geometrical characteristics proved to be a valuable tool in positioning the mode profile in the vertical direction.

Calculations were performed using COMSOL's Finite Elements solver. The evolution of the effective index of the fundamental mode with wavelength was calculated by taking into account the material dispersion. Finally, the contribution of SiGe in each mode profile was estimated by calculating the integral:

$$n = \frac{\iint n(\mathrm{x},\mathrm{y})\left|E\right|^2 dxdy}{\iint \left|E\right|^2 dxdy} \tag{3}$$

where $n(x,y)$ is the material wavelength dependent index over the Si, SiGe plane.

The main factor affecting the waveguide dispersion is the ratio H/L. For a given H value, an increase in L results in a blue shift of the ZDW. The waveguide design targeted in the fabrication was determined following a series of design calculations that aimed at optimizing the dispersion profile for our application. A design with H and L dimensions of 1.536 μm and 1 μm respectively, yielded the dispersion curve plotted in Fig. 1(b) and was eventually chosen to be fabricated. The nonlinear coefficient n_2 of this waveguide was estimated to be $1.28\text{x}10^{-13}$ cm^2/W at 2 μm, which relates directly to an estimated mean Ge concentration value of x = 0.08 for the fundamental TM mode [6]. According to previous estimations [6], the n_2 value for pure silicon is $1.04\text{x}10^{-13}$ cm^2/W at the same wavelength. The low value of x represents a compromise in the nonlinearity of the waveguide [8], and is due to a high δ value in this structure (δ = 1 μm). However, a higher x value (or smaller δ value) would result in a

#205974 - $15.00 USD Received 4 Feb 2014; revised 3 Apr 2014; accepted 3 Apr 2014; published 15 Apr 2014

ZDW that would lie further in the infrared, and consequently in unfavorable phase matching conditions. The phase matching diagram associated to this dispersion profile can be evaluated as shown in Fig. 1(c). The diagram shows the formation of the two gain bands when pumping the waveguide in the normal dispersion region, which allows broadband conversion and the translation of mid-IR wavelengths to the near-IR.

2.2 Waveguide fabrication

The SiGe waveguide structure was grown by reduced pressure chemical vapor deposition on a SOI (silicon on insulator) wafer with 2µm buried oxide layer (Box). A buffer Si layer was first grown to adjust the SOI layer thickness to the desired value ($S + \delta$). The linear gradient in germanium concentration on the waveguide profile was then achieved by varying the germane mass-flow during growth of the SiGe layer while keeping the dichlorosilane mass-flow constant [12]. As a result, the concentration of Ge in the SiGe layer was linearly increased from 0% to 42% and then decreased back to pure Si symmetrically, as shown in Fig. 1(a). The top of the SiGe graded index layer was lowered by etching while monitoring in situ the Ge content in the etched by-products with mass spectroscopy. The process was stopped when the SiGe concentration was such that yielded the appropriate H value of 1.536 µm. Then the waveguide was realized by photolithography and etching. Etching ensured that the thickness of Si on the box layer that constituted the slab was 210 nm. Figure 2(a) shows a scanning electron microscopy (SEM) image of the fabricated waveguide cross-section. The image shows that there was an actual sidewall angle leading to a trapezoidal shape with a top width of 1 µm whereas the bottom width was about 1.289 µm. The main influence of this shape on the optical properties of the waveguide is a slight red shift of the zero dispersion wavelength by 5 nm.

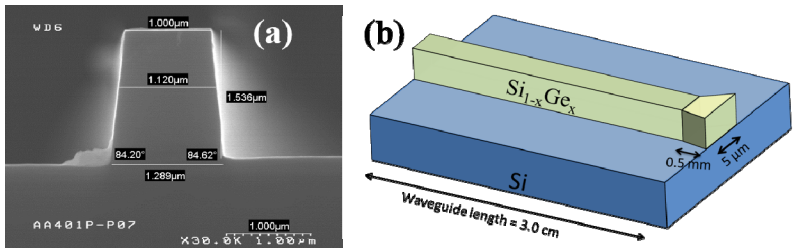

Fig. 2. (a) Scanning Electron Microscopy (SEM) image of the SiGe waveguide, (b) Sketch of the SiGe waveguide

In order to optimize the launching efficiency, a 5-µm width taper was added at the input of the 3-cm long waveguide [see Fig. 2(b)]. A characterization of the waveguide showed that it exhibited losses close to 2 dB/cm, whereas the simulations predicted a nonlinear coefficient of 36 /W/m at 2 µm, a value which was also verified experimentally through a measurement of the nonlinear phase shift of a dual-frequency beat signal [8].

3. Experimental results

3.1 Experimental setup

The experimental setup is shown in Fig. 3. The wavelength conversion experiments were carried out using two single-frequency broadly tunable CW lasers (IPG Photonics) operating in the vicinity of 2 µm. The first, used as the pump, was tunable between 2.0 and 2.5 µm whereas the second, used as the signal, could be tuned from 2.0 to 2.8 µm. A beam-splitter adapted to the laser wavelengths was used to couple together the signal and pump. Two waveplates were used to control the input polarization into the waveguide. The light was coupled into the waveguide through a combination of a CaF_2 lens (transparent up to 8 µm)

#205974 - $15.00 USD Received 4 Feb 2014; revised 3 Apr 2014; accepted 3 Apr 2014; published 15 Apr 2014

and a lensed fiber, and was collected at the output by a mid-IR objective. The output signal was measured on an optical spectrum analyzer (OSA) which operated up to 2.4 µm.

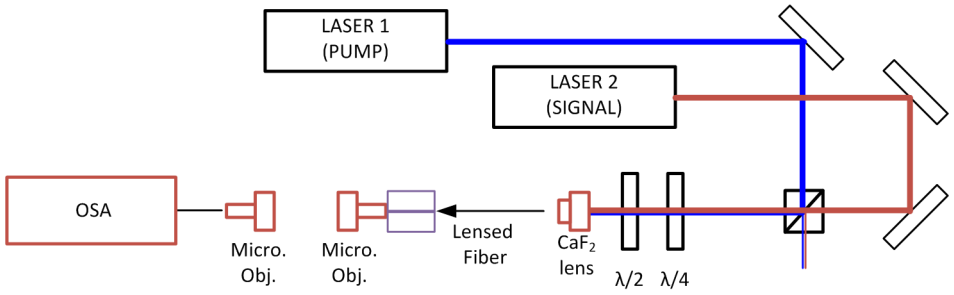

Fig. 3. Experimental setup.

3.2 ZDW and typical spectra

First, the calculated phase matching curve was verified through a series of tests that used signals centered at four successive wavelengths, namely 2290 nm, 2340 nm, 2400 nm and 2640nm. The pump wavelength leading to the highest conversion efficiency for each of these signal wavelengths was recorded as 2160 nm, 2151.7 nm, 2143.2 nm and 2122 nm respectively. These wavelength values are in good agreement with the theoretical phase matching diagram [see symbols in Fig. 1(c)]. This confirms that the ZDW was close to 2135 nm as expected from the numerical modeling.

Figure 4 reports the spectra obtained when a pump centered at 2122 nm was used and the signal wavelength was varied. Figure 4(a) shows the converted idler for a signal centered close to the limit of the OSA. Note that the conversion efficiency reading on the OSA, here –25 dB, does not represent a real value because the collecting optics and fiber exhibited a higher loss at longer wavelengths. Figure 4(b) presents one of the broadest wavelength conversion obtained for a signal at 2650 nm to an idler at 1771 nm.

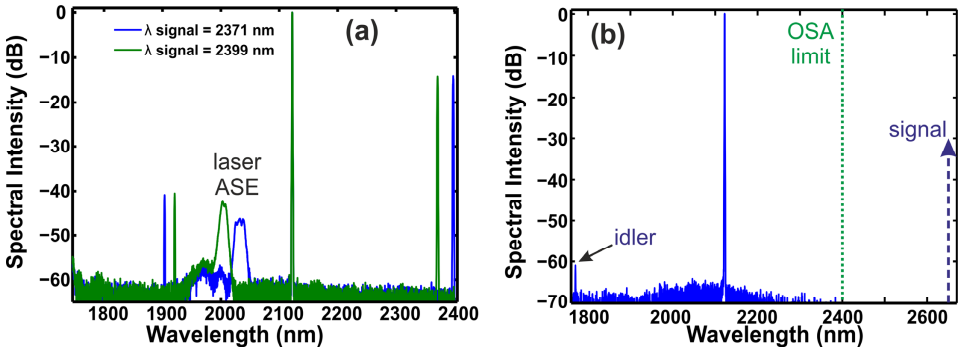

Fig. 4. (a) Spectra for a signal at 2371 nm (green line) and at 2399 nm (blue line). (b) Spectra obtained for a signal centered at 2650 nm. For both spectra, the pump wavelength is 2122 nm.

3.3 Conversion efficiency

The conversion efficiency (CE), defined here as $P_{idler}(output)/P_{Signal}(output)$ was recorded for a wavelength sweep over the tunable range of the signal laser while keeping the pump wavelength constant at 2122 nm. The conversion efficiency values were deduced either directly from the OSA for signal wavelengths up to 2.4 µm or, at longer wavelengths, measured with the use of a power meter. In both cases, the losses at longer wavelengths of the optical components that were placed after the waveguide (i.e. lens, objectives and fibers) were carefully estimated as a function of the wavelength and taken into account in the CE

#205974 - $15.00 USD Received 4 Feb 2014; revised 3 Apr 2014; accepted 3 Apr 2014; published 15 Apr 2014

calculations. (It was verified during the experiment that the measured signal power remained unaffected by the presence of the pump.)

Figure 5 summarizes our measurements and compares them with numerical simulations which considered an input launched power of 75 mW for the pump and 10 mW for the signal, and waveguide losses of 2 dB/cm, in line with the experimental values. The simulations were conducted with the use of nonlinear propagation equations first appearing in [13]. The model accounted for the propagation losses, the two photon absorption and the free carrier absorption effects, the wavelength dependence of n_2 and two photon absorption and the cross nonlinearity parameters calculated following the methodology of [13] after the adaptation of the nonlinear parameters in accordance with the methodology in [6]. However, it was found that the nonlinear losses could be neglected for the pump powers considered in our experiments (lower than 100 mW).

The comparison is in qualitative agreement. The difference between the experimental and numerical data can be attributed to several factors, such as the exact dispersion characteristics of the waveguide. As an example, we show in Fig. 5 the difference that a shift of just + 6 nm (green dashed line) or −6 nm (red dashed line) in the ZDW would make to the wavelength conversion performance.

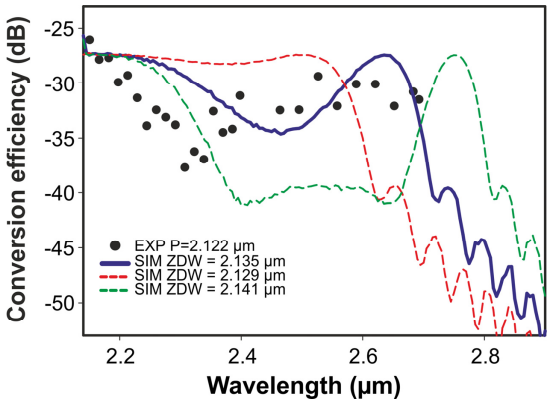

Fig. 5. Conversion efficiency as a function of the signal wavelength. Comparison between experiments (black dots) and numerical simulation for the dispersion shown in Fig. 2(a) (blue solid line) and for the zero dispersion shifted of + 6 nm (green dashed line) and - 6 nm (red dashed line).

The figure also demonstrates a CE of −32 dB for the conversion from 2650 nm to 1771 nm, which represents one of the highest values ever reported. Note that it was not possible to demonstrate broader conversion than this due to limitations in the tunability of the lasers used.

4. Conclusion

We have reported the conversion of mid-infrared signals to the near-infrared based on four-wave mixing in a SiGe waveguide. The waveguide used was specially designed for this application, and exhibited a linearly graded concentration in germanium, which allowed both for an enhanced nonlinear performance (as compared to pure Si waveguides) and a tailored ZDW. The broadest conversion we observed was from 2.65 μm to 1.77 μm using a pump at 2.12 μm. The experiment demonstrates that dispersion-engineered SiGe waveguides could lead to the realization of mid-IR spectrometers and high-sensitivity sensors. Obviously, the same technique can be applied for down-conversion as well (as it has already been demonstrated e.g. in PPLN [2, 14] and silicon wires [15, 16]). Down-conversion of signals to mid-IR wavelengths can be appealing for free-space communication applications. It is noted

#205974 - $15.00 USD Received 4 Feb 2014; revised 3 Apr 2014; accepted 3 Apr 2014; published 15 Apr 2014

however, that the efficiency of the conversion would be lower in this case, limited by the onset of two-photon absorption at the signal wavelengths.

Acknowledgments

This work was supported by the European Communities Seventh Frame-work Program FP7/2007-2013 under Grant 288304 (STREP CLARITY).

#205974 - $15.00 USD Received 4 Feb 2014; revised 3 Apr 2014; accepted 3 Apr 2014; published 15 Apr 2014